



Electrochemical and surface analysis study of copper corrosion protection by 1-propanethiol and propyltrimethoxysilane: A comparison with 3-mercaptopropyltrimethoxysilane

R. TREMONT and C.R. CABRERA*

Department of Chemistry, University of Puerto Rico, PO Box 23346, San Juan, Puerto Rico 00931-3346

(*author for correspondence, e-mail: ccabrera@goliath.cnet.clu.edu)

Received 1 June 2001; accepted in revised form 19 March 2002

Key words: copper, corrosion inhibition, propyltrimethoxysilane, 1-propanethiol

Abstract

The inhibition of Cu corrosion by 1-propanethiol (1-PT) and propyltrimethoxysilane (PTS) molecules, in 0.100 mol L⁻¹ KCl solution, was investigated and compared to 3-mercaptopropyltrimethoxysilane (MPS). Corrosion inhibition was studied as a function of the 1-PT and PTS concentration in ethanol, between 1.0 × 10⁻⁷ mol L⁻¹ and 1.0 × 10⁻² mol L⁻¹. Inhibition efficiency was calculated from Tafel plots in 0.100 mol L⁻¹ KCl solution. It improved with an increase in 1-PT or PTS concentration. The maximum efficiency was obtained at a 1-PT or PTS concentration of 1.0 × 10⁻³ mol L⁻¹ or 1.0 × 10⁻⁵ mol L⁻¹, respectively. Adsorption of 1-PT and PTS on copper followed a Langmuir behaviour. Potentiostatic polarization measurements indicated that 1-PT and PTS are mixed anodic/cathodic inhibitors, in the presence of dissolved oxygen. When the inhibitor exposure time of the pretreated Cu surface in 0.100 mol L⁻¹ KCl solution was varied, a loss on the corrosion inhibition efficiency was observed for the three (MPS, PTS and 1-PT) compounds. However, the 1-PT compound maintained excellent protection in the first 12 h of exposure to a 0.100 mol L⁻¹ KCl solution; afterwards, there was a significant loss in the inhibition efficiency. Surface analysis studies with Auger electron spectroscopy (AES), X-ray photoelectron spectroscopy (XPS), and scanning electron microscopy (SEM) showed that the inhibitors modified the Cu surface.

1. Introduction

Copper is a metal that has been widely used in different types of industries, including electronic, due to its high corrosion resistance. Its protection against corrosion avoids large costs on reparations and equipment replacements. In spite of copper being a relatively noble metal, it reacts easily in oxygen containing environments. Since copper and its alloys are not stable in oxygen-containing electrolytes, substantial improvement in their passivity is needed. This can be achieved by the use of organic compounds as corrosion inhibitors. The chemisorption of alkanethiols and silanes molecules over copper has been placed to practice by several research groups [1–35]. Benzenethiol and some of its derivatives have shown to be very effective as copper corrosion inhibitors in acid and alkaline solutions. Other compounds presented recently include 2-mercaptobenzothiazol, 11-mercapto-1-undecanol, 1,2-bis(trichlorosilil)ethane, and octadecyltrichlorosilane [26, 27].

The thiol, as head functional group, forms a strong covalent bond with different metals [37, 39]. On the other hand, the trimethoxysilane group, which has three methoxy functional groups, is a very effective protector

of metallic surfaces [38, 39] against corrosion. TrabANELLI attributed this behavior of protection to a film formation on the metal surface [26]. In our previous work [40] we reported on the inhibition effect of 3-mercaptopropyltrimethoxysilane (MPS) on copper corrosion in 0.100 mol L⁻¹ KCl solution. We observed 95% corrosion inhibition efficiency for an optimum MPS pretreatment concentration of 1.0 × 10⁻⁴ mol L⁻¹ in ethanol. The FTIR data indicated the presence of a polymer on the Cu surface [41–48]. During the surface modification, there is a partial disappearance of the –SiOCH₃ and –SiOC FTIR signals and the appearance of a –Si–O–Si– stretching band [49–52]. This could be due to the presence of partial polymerization of the MPS molecules or –SiOCH₃ or Si–OH defects in the polymer. Furthermore, the –SH signal disappeared, which suggest that the MPS chemisorption onto the Cu surface is through the sulfur atom [50].

In this paper, the Cu corrosion inhibition properties of propyltrimethoxysilane (PTS) and 1-propanethiol (1-PT) molecules in 0.100 mol L⁻¹ KCl solution are discussed. In addition, they are compared with the 3-mercaptopropyltrimethoxysilane (MPS) molecule. The structures of the three molecules are shown in Figure 1.

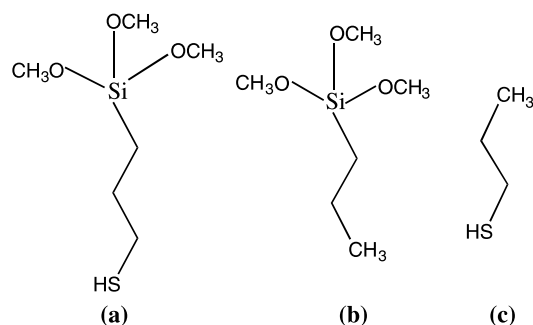


Fig. 1. Chemical structure of (a) 3-Mercaptopropyltrimethoxysilane (MPS), (b) propyltrimethoxysilane (PTS) and (c) 1-propanethiol (1-PT).

The corrosion inhibition process of these molecules has been studied by applying potential polarization curves, polarization resistance measurement, Auger electron spectroscopy (AES), X-ray photoelectron spectroscopy (XPS) and scanning electron microscopy (SEM).

2. Experimental details

Sheets of Cu (foil of 1.0 mm, Aldrich, 99.98%) of 1 cm² in geometric area were used in all experiments. Before be used, the sheets were mechanically polished with a silicon carbide belt (from 240 grit to 600 grit, Buehler), rinsed with nanopure water (18 MΩ cm), polished with diamond paste (1 μm, Buehler) using a microcloth polishing cloth (Buehler), rinsed with acetone (Aldrich) and, finally, dried under nitrogen. The freshly polished electrodes were pretreated before each experiment by cleaning with 10% HCl (Aldrich) for 30 s and washing with nanopure water.

The Cu electrode surface chemical pretreatment was done by immersing the Cu surface in 30 mL ethanol solution with different PTS and 1-PT (95%, Aldrich) concentrations, ranging from 1.0 × 10⁻² mol L⁻¹ to 1.0 × 10⁻⁷ mol L⁻¹, and at different exposure times, ranging from 30 min to 3 h. The surfaces were then rinsed with ethanol and nanopure water, dried under nitrogen, and immersed in a 0.100 mol L⁻¹ KCl solution between 1 h and 8 h for further studies.

The temperature in all the experiment was 23.6 ± 0.1 °C and the KCl solutions had a pH of 6.3 ± 0.1. The experiments were done in the presence of air.

The electrochemical measurements were performed in a conventional three-electrode electrochemical cell. Consisting of Cu metal as the working electrode, a platinum electrode, as an auxiliary electrode, and a saturated calomel electrode (SCE), as the reference. A Princeton Applied Research (PAR) 273A potentiostat/galvanostat, controlled with a PAR 270 Research Electrochemistry Software installed in a personal computer, was used in our experiments.

For Auger electron spectroscopy (AES) analysis, a PHI 660 spectrometer was used. This instrument had electron beam energy of 3.0 and 5.0 keV. The X-ray

photoelectron spectroscopy (XPS) analyses presented in this work were performed using a PHI 5600ci spectrometer. For the AES and XPS measurements, the samples were mounted over a stainless steel stopper using a molybdenum mask to ensure good electrical contact. For XPS analysis the sample analyses were done using a MgK_α X-ray source at 15.0 kV and 400 W. This instrument was equipped with a hemispherical analyser. The pass energy used was 93 eV for the survey analysis and 11 eV for the high-resolution studies. All analyses were performed at a vacuum pressure below 1.0 × 10⁻⁹ torr. The binding energy (E_{BE}) values were corrected using the C 1s binding energy signal due to the atmospheric contamination ($E_{BE} = 285.0$ eV).

The scanning electron microscopy (SEM) analysis were done using a Jeol JSM-5800LV with an accelerating voltage between 15.0 kV and 20.0 kV. Samples were attached on top of an aluminium stopper by means of 3M carbon conductive adhesive tape (SPI).

3. Results and discussion

3.1. Effect of the PTS and 1-PT concentration on copper corrosion inhibition

In this study we applied polarization curves to characterize the protection efficiency of PTS and 1-PT on Cu surfaces. Tafel plots in the neighbourhood of the corrosion potential, $E_{corr} \pm 300$ mV, using a 1 mV s⁻¹ potential sweep rate were used for the determination of the corrosion inhibition efficiency.

Polarization curves, graphed as Tafel plots, for Cu, pretreated with different concentrations of PTS, in 0.100 mol L⁻¹ KCl solution are presented in Figure 2A. From the Tafel plots we can obtain the exchange current density for corrosion by extrapolating the Tafel line to the potential of corrosion. The corrosion inhibition efficiency, E_f , with units of percent, were calculated from the following equation:

$$E_f = \left(\frac{i_o - i}{i_o} \right) \times 100 \quad (1)$$

where i and i_o are the corrosion current densities with and without pretreatment, respectively. From these measurements the optimum chemical pretreatment can be determined. For PTS the pretreatment concentration for the copper corrosion inhibition in 0.100 mol L⁻¹ KCl solution was 1.0 × 10⁻⁵ mol L⁻¹. This gave an efficiency of 84%. The corrosion potential, E_{corr} , shifted towards more noble values in presence of PTS. The shift of E_{corr} could be explained by the fact that the inhibitor had a stronger influence on the copper dissolution reaction than on the cathodic oxygen reduction [57].

Figure 2B shows I_{corr} against log C_{PTS} plot for Cu electrodes at different PTS concentration. A current density maximum for the corrosion inhibition, and an

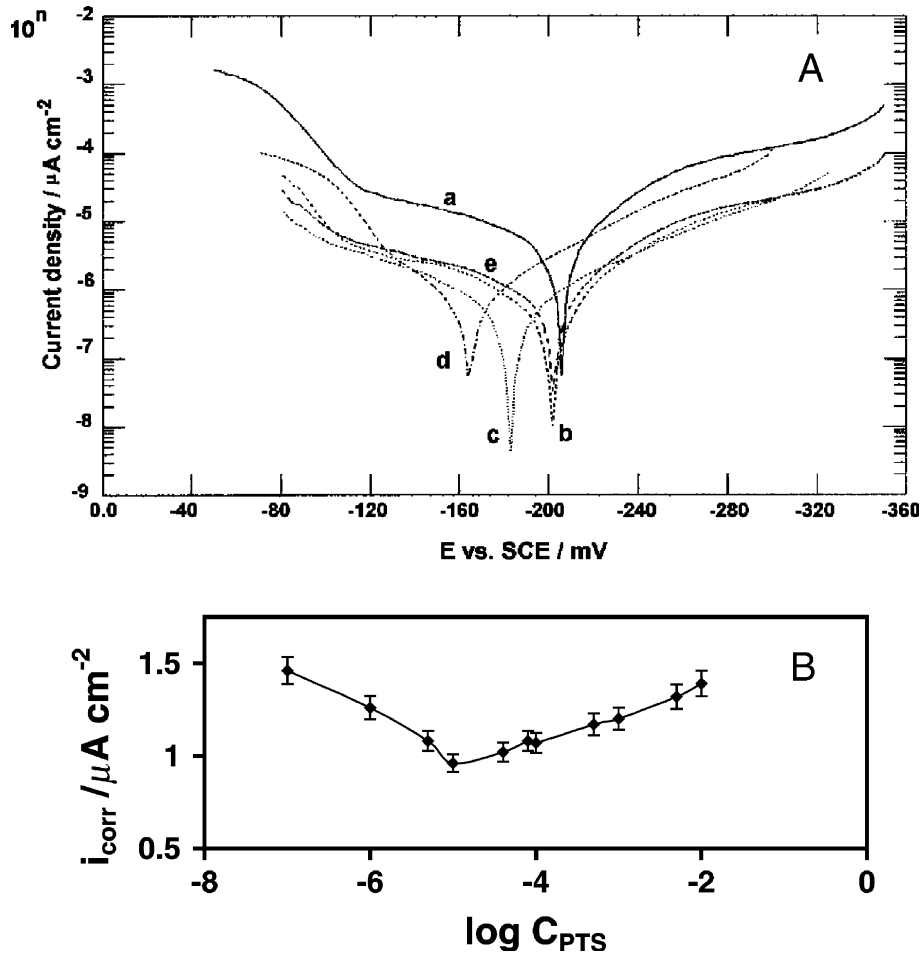


Fig. 2. (A) Tafel plots from polarization curves made to Cu electrodes in 0.100 mol L^{-1} KCl that had different pretreatment concentrations of PTS (C_{PTS}). (a) Without PTS pretreatment; with pretreatment PTS concentrations of (b) $1.0 \times 10^{-7} \text{ mol L}^{-1}$; (c) $1.0 \times 10^{-5} \text{ mol L}^{-1}$; (d) $1.0 \times 10^{-3} \text{ mol L}^{-1}$ and (e) $1.0 \times 10^{-2} \text{ mol L}^{-1}$. (B) i_{corr} against $\log C_{\text{PTS}}$.

apparent dependence of I_{CORR} on bulk concentration, was observed for copper.

The pretreatment with 1-PT compound showed a better Cu corrosion inhibition efficiency in 0.100 mol L^{-1} KCl solution. In Figure 3 it is observed that the optimum pretreatment concentration is 1.0×10^{-3}

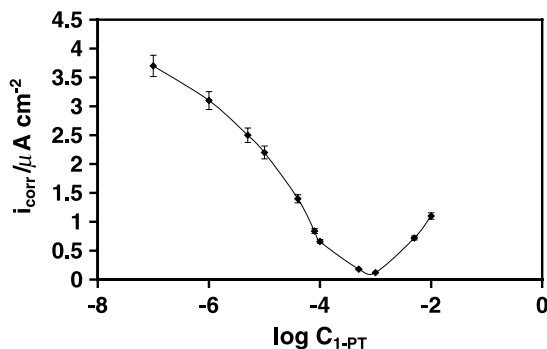


Fig. 3. Plot of i_{corr} against $\log C_{1\text{-PT}}$ curve of a Cu electrode in 0.100 mol L^{-1} KCl at different pretreatment concentrations of 1-PT for 30 min. The electrode was placed in the KCl solution for 1 h before the polarization measurements. The corrosion current, i_{corr} , was obtained from the Tafel plots.

mol L^{-1} , with an efficiency of 98% (see Table 1). The E_{CORR} is moved about 20 mV towards the cathodic zone; however, as the pretreatment concentration was increased, the E_{CORR} varied without following a trend.

A comparison on the polarization resistance (R_p) calculated values with respect to the $\log C$ for PTS and 1-PT used in the chemical pretreatment, is shown in Figure 4. The R_p value was calculated from a plot of $E(\text{V})$ against i ($R_p = \Delta E/\Delta I$) near the corrosion potential (i.e., $E_{\text{CORR}} \pm 20 \text{ mV}$). As can be seen from Figure 4, the R_p value increases with an increase on the chemical pretreatment concentration, achieving a maximum R_p of $68 \text{ k}\Omega \text{ cm}^{-2}$ at a PTS concentration of $1.0 \times 10^{-5} \text{ mol L}^{-1}$. However, for the inhibitor 1-PT the optimum concentration was $1.0 \times 10^{-3} \text{ mol L}^{-1}$ for an efficiency of 98%.

A comparison of the corrosion inhibition efficiencies for the chemical pretreatment materials, MPS, PTS, and 1-PT, in 0.100 mol L^{-1} KCl solution is shown in Figure 5. It is observed that the optimum efficiency for each inhibitor was at different concentrations. For MPS the chemical pretreatment at low concentrations had very small efficiency. However, MPS surface modification improves the corrosion inhibition efficiency as the

Table 1. Corrosion parameters for copper in 0.1 M KCl with and without the addition of inhibitor as obtained by the Tafel plot from polarization measurements

Inhibitor /mol L ⁻¹	PTS						1-PT					
	E_{corr} /mV vs SCE	I_{corr} / $\mu\text{A cm}^{-2}$	β_{c} /V dec ⁻¹	β_{a} /V dec ⁻¹	E /%	R_{p} /k $\Omega \text{ cm}^{-2}$	E_{corr} /mV	I_{corr} / $\mu\text{A cm}^{-2}$	β_{c} /V dec ⁻¹	β_{a} /V dec ⁻¹	E /%	R_{p} /k $\Omega \text{ cm}^{-2}$
0	-206	6.00	-125	52	—	17	-206	6.00	-125	52	—	17
1×10^{-7}	-203	1.46	-71	128	76	42	-203	3.70	-88	90	38	23
1×10^{-6}	-202	1.26	-58	153	79	51	-182	3.10	-88	87	48	26
5×10^{-6}	-193	1.08	-66	113	82	63	-184	2.50	-88	91	59	32
1×10^{-5}	-183	0.96	-68	80	84	68	-201	2.20	-88	95	64	38
4×10^{-5}	-200	1.02	-68	98	83	65	-186	1.40	-88	89	76	43
8×10^{-5}	-198	1.08	-66	138	82	59	-192	0.84	-88	87	87	53
1×10^{-4}	-164	1.12	-57	52	81	58	-194	0.66	-88	62	89	69
5×10^{-4}	-184	1.20	-64	76	80	51	-223	0.18	-88	71	97	76
1×10^{-3}	-164	1.18	-69	170	79	48	-230	0.12	-88	77	98	84
5×10^{-3}	-203	1.32	-68	162	78	38	-203	0.72	-87	68	88	66
1×10^{-2}	-202	1.39	-68	141	77	33	-190	1.10	-86	63	82	59

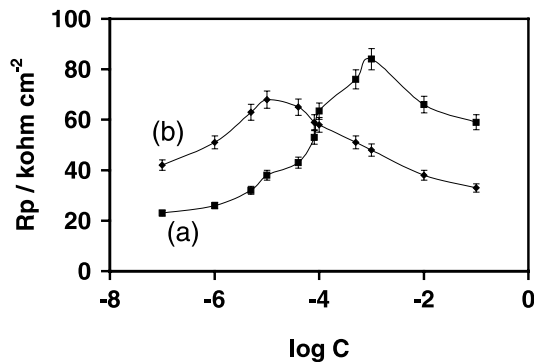


Fig. 4. Variation of the charge transfer resistance (R_p) of the Cu modified electrodes as a function of the $\log C$ for (a) 1-PT and (b) PTS used in the pretreatment process. After the pretreatment, the electrodes were placed in 0.100 mol L⁻¹ KCl solution for 1 h prior to the polarization measurements. The C (mol L⁻¹) is the PTS and 1-PT concentration used in the pretreatment of the Cu electrodes.

concentration is increases until reaching a maximum of 95% at a chemical pretreatment concentration of 1×10^{-4} mol L⁻¹. However, PTS shows better efficiency at low concentrations, maintaining a constant value when increasing the pretreatment concentration. This compound maintains a corrosion inhibition efficiency over 75%, which makes it reliable for copper protection in the KCl solution under study. On the other hand, the 1-PT compound has an efficiency, at low concentrations, of about 40%. This value increases slowly with increasing concentration of 1-PT until reaching a maximum efficiency of 98% at a chemical pretreatment concentration of 1.0×10^{-3} mol L⁻¹.

Values for the corrosion potential (E_{corr}), corrosion current density (i_{corr}), efficiency (E) and polarization resistance (R_p), as a function PTS and 1-PT concentration in an aqueous 0.100 mol L⁻¹ KCl solution are presented in Table 1. As it can be observed, the 1-PT compound maintains a constant cathodic (β_{c}) and anodic slope (β_{a}) with concentration. The PTS compound shows variations in the interaction mechanisms

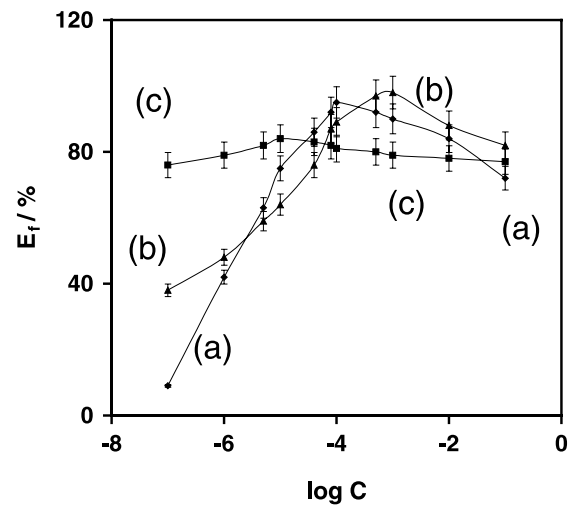


Fig. 5. Comparison of the inhibition efficiency (E_r) variation of copper corrosion in 0.100 mol L⁻¹ KCl as a function of $\log C$ for (a) MPS, (b) 1-PT and (c) PTS. After the pretreatment, the electrodes were placed in 0.100 mol L⁻¹ KCl solution for 1 h prior to the polarization measurements. The C (mol L⁻¹) is the MPS, PTS and 1-PT concentration used in the pretreatment of Cu.

in the anodic (β_{a}) and cathodic (β_{c}) zones, with greater emphasis on the anodic zone.

3.2. Effect of the exposure time of the Cu metal in the PTS and 1-PT solution

For this study, the effect of exposure time of the metal to the ethanolic pretreatment solution of PTS and 1-PT of 1.0×10^{-5} mol L⁻¹ and 1.0×10^{-3} mol L⁻¹, respectively. The exposure time to the pretreatment inhibitor solution was varied between 30 min and 8 h. Afterward, the modified Cu plate was placed in 0.100 mol L⁻¹ KCl, for 1 h, prior to the electrochemical measurements.

Polarization studies in KCl solution were done to determine the corrosion current density. Figure 6 shows i_{corr} against time plots for Cu electrodes at different exposure times in PTS/ethanol or 1-PT/ethanol pre-

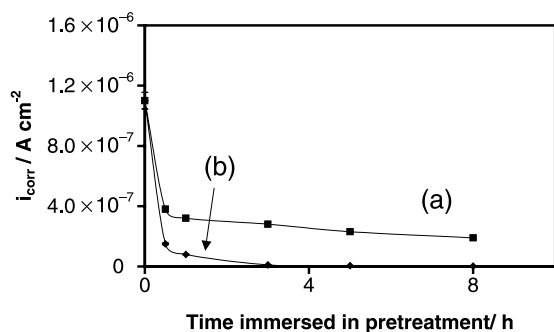


Fig. 6. Plot of i_{corr} against time for Cu electrodes in 0.100 mol L^{-1} KCl. Previously placed for 1 h in the KCl solution. The electrodes were pretreated with (a) PTS ($1.0 \times 10^{-5} \text{ mol L}^{-1}$) ethanolic solution and (b) 1-PT ($1.0 \times 10^{-3} \text{ mol L}^{-1}$) ethanolic solution with different exposure times. The corrosion current, i_{corr} , was obtained from the Tafel plots obtained from the polarization curves.

treatment solution and after one hour of exposure to a 0.100 mol L^{-1} KCl solution. Curve 6(a) shows the case for PTS ($1.0 \times 10^{-5} \text{ mol L}^{-1}$) compound pretreatment of the Cu surface. We observed that the minimum corrosion current density was at 8 h of exposure to PTS, showing an inhibition efficiency of 92%. In curve 6(b), for the Cu pretreatment with 1-PT, the optimal concentration was $1.0 \times 10^{-3} \text{ mol L}^{-1}$. The maximum observed protection of the copper surface, at 99%, was reached after 3 h of exposure to the 1-PT pretreatment solution. This electrode showed had a better efficiency than in the case of PTS, at shorter exposure times to the ethanolic pretreatment solution. It is our understanding that the 1-PT molecules can be aligned more easily than PTS and a greater amount of 1-PT, per surface area, can be adsorbed on the Cu surface. Therefore, improving the corrosion inhibition efficiency. Tremont et al. [40] reported similar results for MPS, with an optimal pretreatment concentration of $1.0 \times 10^{-4} \text{ mol L}^{-1}$ and maximum protection of 98%. The exposure time to the pretreatment MPS solution was 3 h.

3.3. Effect of the exposure time in 0.100 mol L^{-1} KCl solution of the Cu/inhibitor surface

In this study the copper electrode was placed in the ethanolic pretreatment solution at the experimentally determined optimal concentration for each inhibitor and exposure pretreatment time. The Cu electrode was placed in contact with ethanolic solutions of 1-PT ($1.0 \times 10^{-3} \text{ mol L}^{-1}$ for 3 h) or PTS ($1.0 \times 10^{-5} \text{ mol L}^{-1}$ for 5 h). Afterward, the exposure time to the corrosive environment, that is, 0.100 mol L^{-1} KCl solution, was varied up to 24 h (Figure 7). In the 1-PT case (curve 7(a)) we observed that in the first 12 h of exposure to the KCl solution there are no significant variations in the corrosion current density. Curve 7(b) shows i_{corr} against time for the PTS pretreated Cu electrodes. We observed that as the exposure time in the KCl solution increases, the corrosion current density increases up to a constant i_{corr} value.

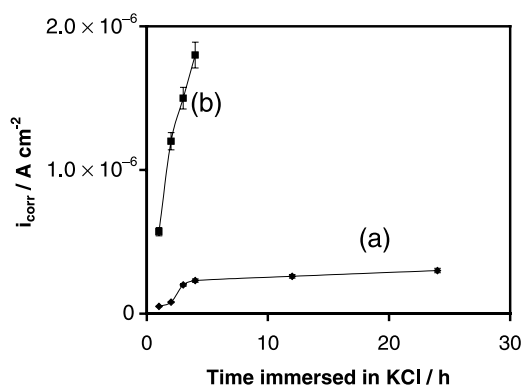


Fig. 7. Plot of i_{corr} against time for Cu electrodes at exposure time (a) of 3 h in 1-PT ($1.0 \times 10^{-3} \text{ mol L}^{-1}$) ethanolic solution and (b) of 5 h in PTS ($1.0 \times 10^{-5} \text{ mol L}^{-1}$) ethanolic solution. Afterward the electrodes were placed at different exposure time in 0.100 mol L^{-1} KCl. The corrosion current, i_{corr} , was obtained from the Tafel plots obtained from the polarization curves.

For the MPS we observed an efficiency loss when increasing the exposure time in the 0.100 mol L^{-1} KCl solution [40].

3.4. Application of the Langmuir adsorption isotherm

Adsorption of an organic adsorbate on a metal surface (Bockris–Swinkels isotherm) is regarded as a substitutional adsorption process between the organic molecule in the aqueous solution ($\text{Org}_{(\text{sol})}$), and water molecules adsorbed on metallic surface ($\text{H}_2\text{O}_{(\text{ads})}$) [58]:

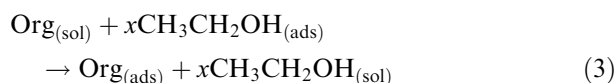


where x is the size ratio, representing the number of water molecules replaced by one molecule of organic adsorbate.

In the Frumkin, Hill de Boer, Parsons, and Temkin isotherms, $x = 1$, and the molecular interaction parameter, a , is included. It depends upon the interaction among the adsorbed molecules and the interaction between metal surface and adsorbate [59]. A positive a value corresponds to attraction and negative a to repulsion [60]. These isotherms assume that the free energy of adsorption ($\Delta G_{(\text{ads})}$) varies linearly with θ . When the absolute value of the free energy of adsorption $|\Delta G_{(\text{ads})}|$ increases, a is positive, when $|\Delta G_{(\text{ads})}|$ decreases, a is negative [61].

The above isotherms can be simplified to the Langmuir isotherm where $a = 0$ and $x = 1$ (Equation 3).

In this work the solvent used was ethanol ($\text{CH}_3\text{-CH}_2\text{OH}$). Therefore, we assumed that an ethanol molecule is replaced by one molecule of organic adsorbate on Cu surface. If we apply the Bockris–Swinkels isotherm we can use the ethanol concentration of 15.52 mol L^{-1} . The mechanism will be similar to that in water:



The adsorption of MPS, PTS and 1-PT on Cu was model using the Langmuir isotherm, $a = 0$ and $x = 1$,

$$\theta = \frac{kC}{(1 + kC)} \quad (4)$$

where C is inhibitor concentration, k is a constant and θ is the surface coverage which is also given by

$$\theta = \frac{E_f}{100} \quad (5)$$

From Equation 4 we obtain

$$\log\left(\frac{\theta}{1-\theta}\right) = \log k + \log C \quad (6)$$

In Figure 8 we have a θ against C plot, which was used to test for Langmuir behaviour. The surface coverage, θ , was calculated using Equation 5 [58, 62]. The three molecules followed closely a Langmuir adsorption isotherm. The k value can be obtained from a $\log [\theta/(1-\theta)]$ against $\log C$ plot. From the k value (the ordinate intercept in Equation 6) we can calculate the free energy of adsorption of MPS, PTS and 1-PT on Cu, knowing that [62]

$$k = A \exp\left(\frac{-\Delta G}{RT}\right) \quad (7)$$

where A (L mol^{-1}) is $1/(\text{solvent concentration})$. As we said above, in our case the ethanol concentration is 15.52 mol L^{-1} . The free energy of adsorption for MPS, PTS and 1-PT was found to be -35 kJ mol^{-1} , -25 kJ mol^{-1} and -32 kJ mol^{-1} , respectively. Values of $-\Delta G_{(\text{ads})}$ of the order of 20 kJ mol^{-1} or lower are

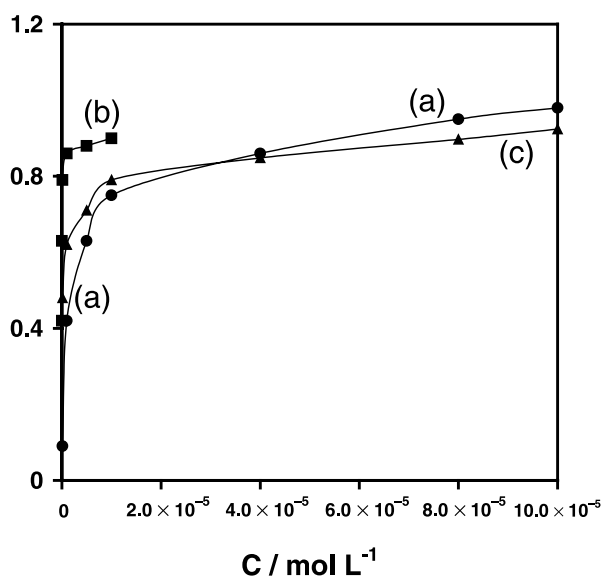


Fig. 8. A comparison of Langmuir adsorption isotherm of (a) MPS, (b) 1-PT and (c) PTS on copper electrodes. Calculated Tafel plots of polarization measurements done in 0.100 mol L^{-1} KCl solution.

generally consistent with a physisorption. Those higher values involve charge sharing or a transfer from the organic molecules to the metal surface to form a coordinate type of bond [63, 64]. This is what we observed for the MPS, PTS, and 1-PT. Nevertheless, we have to consider that the approximations made by Bockris and Swinkels were for aqueous and not ethanolic solutions.

4. Surface analysis studies

Surface analysis studies were done to the Cu electrodes pretreated with the organic compounds. The surfaces studies were; Cu surface exposed to a $1.0 \times 10^{-4} \text{ mol L}^{-1}$ MPS solution for 3 h, or $1.0 \times 10^{-5} \text{ mol L}^{-1}$ PTS for 5 h, or $1.0 \times 10^{-3} \text{ mol L}^{-1}$ 1-PT for 3 h. Additional analyses were done after the chemically modified Cu electrodes were exposed to a 0.100 mol L^{-1} KCl solution for 1 h.

4.1. Auger electron spectroscopy studies

Auger electron spectroscopy (AES) technique was used to determine the presence and elemental composition of the MPS, PTS, and 1-PT molecules on the copper surface.

Figure 9 shows an Auger electron spectroscopy (AES) spectra (a) of a cleaned copper surface used for the chemical surface modification. From the figure we observed Auger peaks for carbon (environment contamination) and Cu only. The cleaning process is needed to eliminate oxides of the copper surface. Figure 9(b) and (c) present the AES of the Cu/MPS (the Cu surface was exposed in $1.0 \times 10^{-4} \text{ mol L}^{-1}$ for 3 h) surface without (b) and with (c) exposure to a solution of 0.100 mol L^{-1} KCl solution for 1 h. Figure 9(d) and (e) present the AES of the Cu/PTS (the Cu surface was exposed in $1.0 \times 10^{-5} \text{ mol L}^{-1}$ for 5 h) and Cu/1-PT (the Cu surface was exposed in $1.0 \times 10^{-3} \text{ mol L}^{-1}$ for 3 h) electrodes without exposed to the KCl solution. From these AES spectra, the elemental composition of the modified Cu surface was obtained (Table 2).

To determine if there were any decomposition of the inhibitor molecules on the copper surface, the atomic ratio between the elements were obtained. This was done by taking the peak area ratios of the AES peaks before applying derived to the signals in the spectra. From Table 2, the atomic ratios found for the MPS pretreated Cu surface were 3.2 for the O/Si atomic ratio (theoretical ratio is 3) and 1.1 for the S/Si atomic ratio (theoretical ratio is 1). The C/O ratio of 1.7 (theoretical ratio is 2), predicts that the oxide species increase the oxygen content on the surface.

4.2. X-ray photoelectron spectroscopy (XPS) studies

X-ray photoelectron spectroscopy was used to characterize the Cu surface under study. Figure 10 shows a

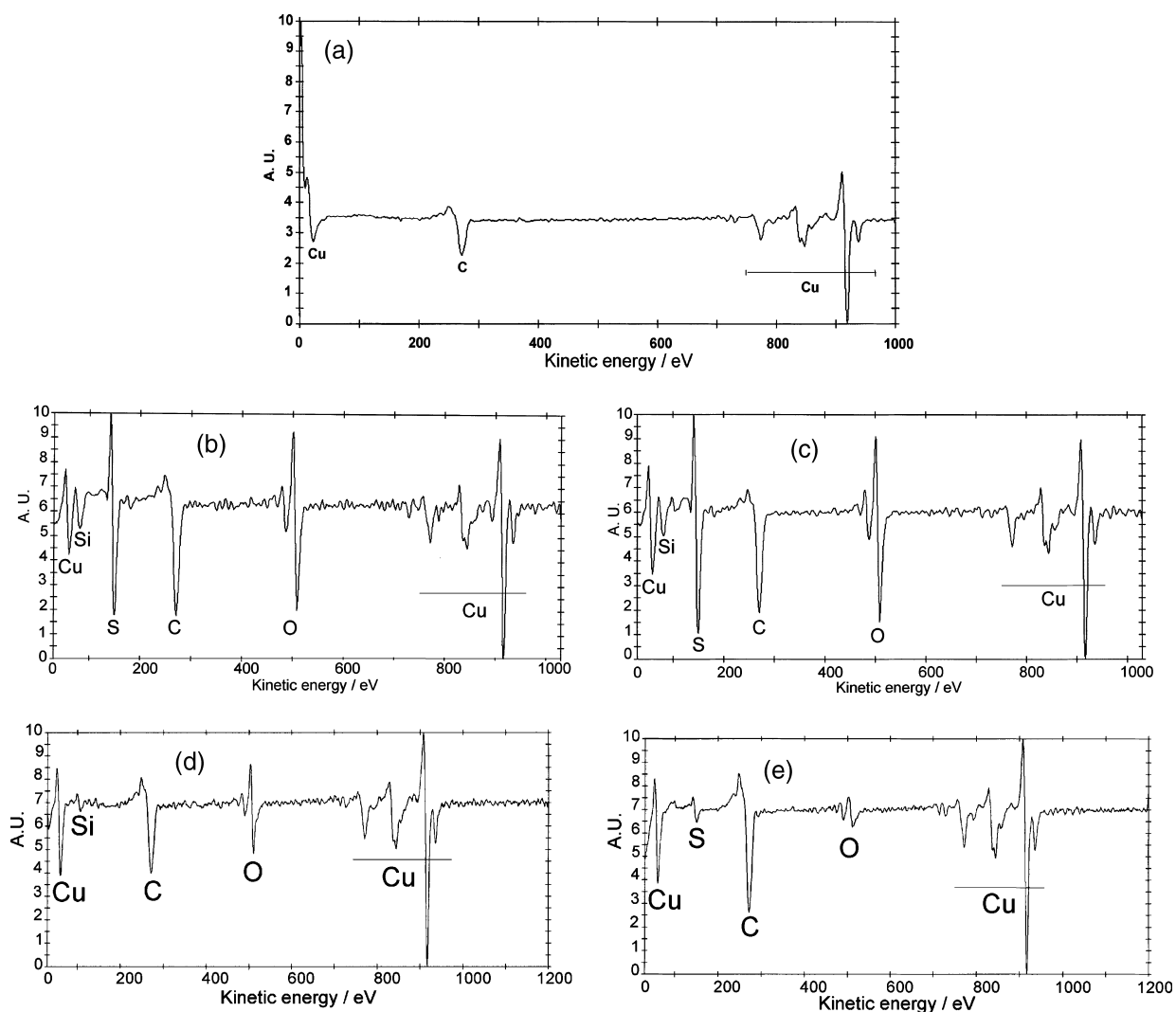


Fig. 9. Auger electron spectroscopy (AES) spectra of (a) a Cu surface without exposure to KCl solution. Cu electrode pretreated with MPS ($1.0 \times 10^{-4} \text{ mol L}^{-1}$ for 3 h) (b) before and (c) after exposed for 1 h in 0.100 mol L^{-1} KCl solution. Cu pretreated electrode with (d) PTS ($1.0 \times 10^{-5} \text{ mol L}^{-1}$ for 5 h) and (e) 1-PT ($1.0 \times 10^{-3} \text{ mol L}^{-1}$ for 3 h). Cu/PTS and Cu/1-PT samples were not exposed to KCl solution.

Table 2. Atomic concentration values (%) and atomic ratio for inhibitor-modified copper surfaces from AES spectra, without exposure to 0.100 mol L^{-1} KCl solution

Element	MPS Concentration /%	PTS Concentration /%	1-PT Concentration /%
C1	29.1	31.4	49.1
O1	17.5	19.1	5.9
S1	5.6	–	12.2
Si1	5.3	6.8	–
Cu1	42.5	42.7	32.8
O/S	3.1 (3)*	–	–
O/Si	3.2 (3)*	2.8 (3)*	–
S/Si	1.1 (1)*	–	–
C/O	1.7 (2)*	1.6 (2)*	–

* Numbers within parenthesis represent theoretical values. Spaces (–) in target within the Table do not have numerical relations.

comparison of high-resolution XPS analyses for Cu ($2p_{1/2}$ and $2p_{3/2}$) regions for different Cu surfaces. The binding energy regions for Cu $2p_{1/2}$ and Cu $2p_{3/2}$, for the

Cu pretreated with MPS, PTS, and 1-PT, before and after being exposed to a solution of 0.100 mol L^{-1} KCl, are presented in Figure 10A. As it is observed in Figure 10A, the 1-PT compound presents the smallest signal for Cu, followed by the MPS pretreated Cu surface. The satellite signal ($\sim 945 \text{ eV}$) produced by the presence of the Cu^{2+} (CuO), is not observed clearly. Figure 10B presents the satellite signal, indicating the presence of CuO species. The binding energy for Cu with PTS compound increases abruptly when exposed to KCl solution, which could be explained possibly by the dissolution of Cu_2O leaving free the CuO species or by the existence of active sites on the metal surface oxidized by the presence of chloride ions.

4.3. Scanning electron microscopy studies

Scanning electron microscopy of the copper surface with inhibitors, before and after being exposed in 0.100 mol L^{-1} KCl solution are presented in Figure 11. Figure 11(a) and (b) show the surface morphology of a

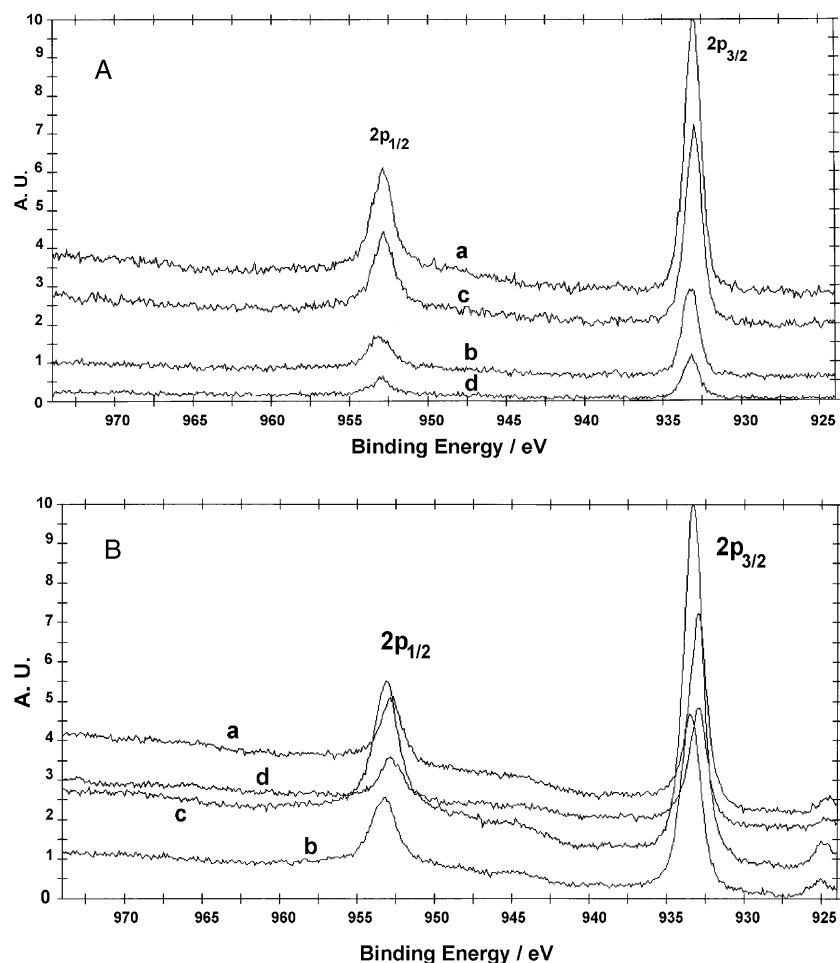


Fig. 10. High resolution X-ray photoelectron spectroscopy (XPS) spectra for the Cu ($2p_{1/2}$ and $2p_{3/2}$) regions. XPS spectra of the Cu-pretreated with inhibitor and (A) without and (B) with exposure to 0.100 mol L^{-1} KCl for 1 h. (a) Without inhibitor; with exposure to (b) MPS ($1 \times 10^{-4} \text{ mol L}^{-1}$ for 3 h); (c) PTS ($1 \times 10^{-5} \text{ mol L}^{-1}$ for 5 h); and (d) 1-PT ($1 \times 10^{-3} \text{ mol L}^{-1}$ for 3 h).

Cu electrode (a) before and (b) after being immersed in 0.100 mol L^{-1} KCl solution for 1 h. The increase of the number of pits is observed on the surface when the Cu is exposed to the attacking KCl solution. The presence of chloride ions and dissolved oxygen helps on the oxidation of the metal.

The micrographs of the Cu surface pretreated with MPS ($1.0 \times 10^{-4} \text{ mol L}^{-1}$ for 3 h) (c) before and (d) after exposed to the KCl solution for 1 h are presented in Figure 11(c) and (d), respectively. The increase of pits on the Cu surface is not as evident as it appeared in Figure 11(b), when it does not have the adsorbed molecule. These micrographs show that the MPS protects the Cu metal surface from the KCl solution.

Figure 11(e) and (f) present the SEM micrographs of the Cu surfaces pretreated with PTS ($1.0 \times 10^{-5} \text{ mol L}^{-1}$ for 5 h) (e) before and (f) after being exposed to 0.100 mol L^{-1} KCl solution for 1 h. From the SEM we observe larger size pits than for the case of the Cu treated with MPS. This result is in agreement with the protection efficiency of the Cu/PTS system, which went to 84% after 1 h of exposure in the KCl solution.

The Cu samples pretreated in a 1-PT ($1.0 \times 10^{-3} \text{ mol L}^{-1}$ for 3 h) solution were analysed by SEM as well.

The micrographs were taken before (Figure 11(g)) and after (Figure 11(h)) being treated with 0.100 mol L^{-1} KCl solution for 1 h. It is observed from the SEMs that the Cu/1-PT had pit formation in active sites when was exposed to KCl solution, but in fewer numbers than in the previous cases.

5. Conclusions

The protection efficiency of the PTS and 1-PT molecules against copper corrosion in 0.100 mol L^{-1} KCl solution was demonstrated varying the concentration of PTS and 1-PT used to protect the copper surface. The optimum concentration for PTS and 1-PT protection of the Cu surface was $1.0 \times 10^{-5} \text{ mol L}^{-1}$ and $1.0 \times 10^{-3} \text{ mol L}^{-1}$, respectively, at room temperature. These compounds, in the presence of oxygen, are mixed anodic/cathodic inhibitors. The effect of PTS and 1-PT protection increases with exposure time in ethanolic solution, containing the inhibitor.

Comparing the three compounds, PTS, 1-PT, and MPS, the PTS compound showed the best efficiency at low concentrations ($1.0 \times 10^{-7} \text{ mol L}^{-1}$) and the MPS

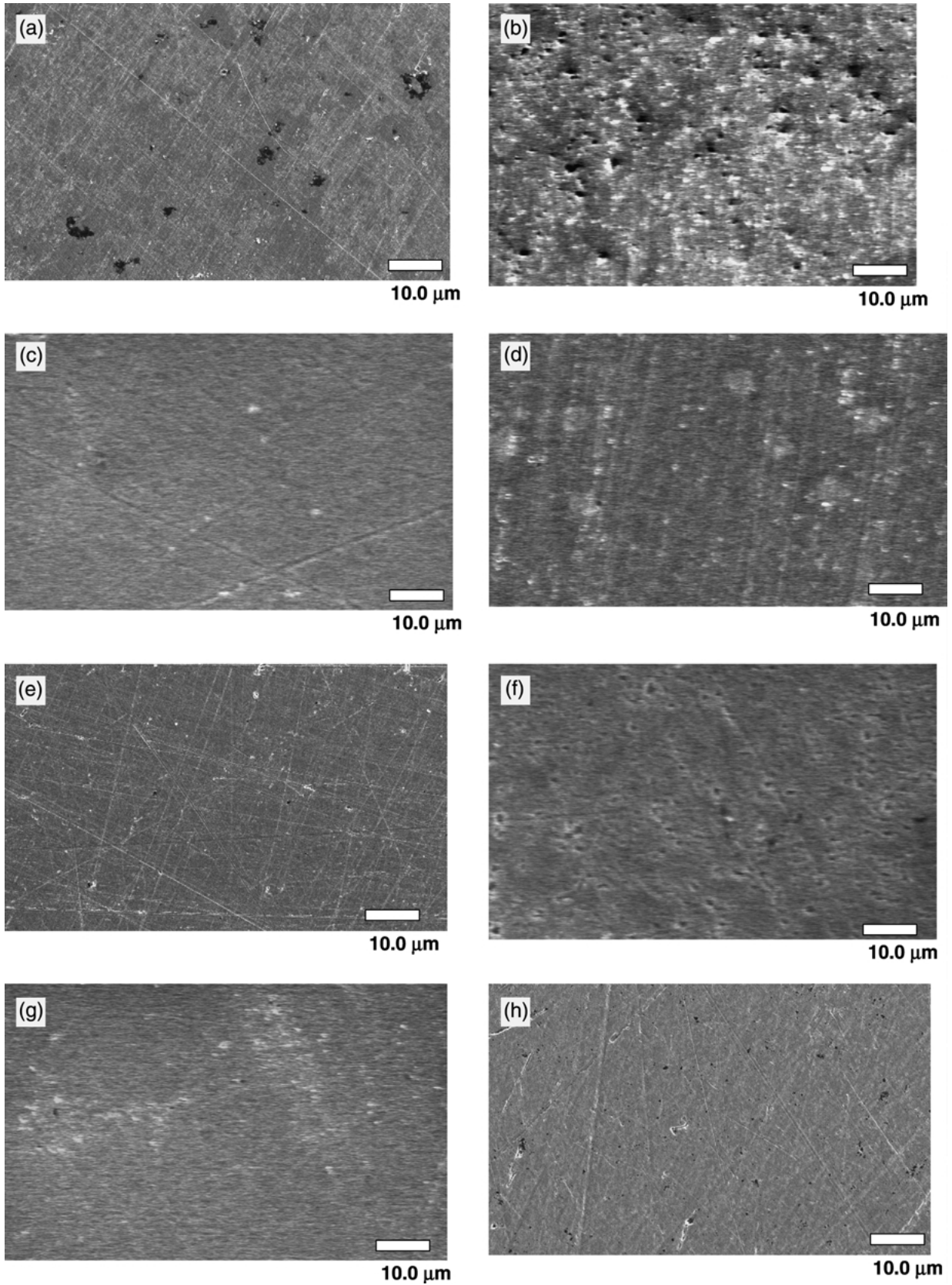


Fig. 11. Scanning electron micrographs (SEM) (4000×) of a copper surface (a) before and (b) after exposure to a 0.100 mol L⁻¹ KCl solution for 1 h. SEM of a copper surface pretreated with MPS for 3 h (c) before and (d) after exposure to a 0.100 mol L⁻¹ KCl for 1 h. SEM of a copper surface pretreated with PTS for 5 h (e) before and (f) after exposure to a 0.100 mol L⁻¹ KCl solution for 1 h. Copper surface pretreated with 1-PT for 3 h (g) before and (h) after exposure to a 0.100 mol L⁻¹ KCl solution for 1 h.

compound had the worst efficiency at these concentration regions. The 1-PT compound showed enhanced corrosion inhibition efficiency at a pretreatment concentration of $1.0 \times 10^{-3} \text{ mol L}^{-1}$ with an exposure time of 30 min. The efficiency was improved when the exposure time was increased in this solution. Compound PTS maintained an efficiency of 92% after 5 h in an ethanol-PTS solution.

When the exposure time of the pretreated Cu surfaces was varied in the 0.100 mol L^{-1} KCl solution, we observed that the three compounds under study lose protection efficiency for copper corrosion inhibition. The 1-PT compound maintained excellent protection in the first 24 h; afterwards the efficiency decreased. The PTS and MPS compounds began to lose corrosion inhibition in the first 2 h of exposure to the 0.100 mol L^{-1} KCl solution.

The AES, XPS, and SEM results support the idea that PTS and 1-PT modifies the Cu surface and inhibits corrosion. The molecules were not decomposed on the Cu surface since the AES atomic ratios were very close to the theoretical ones. The Cu-modified samples, with MPS, PTS, or 1-PT, had pit formation on the surface when they were exposed to the KCl solution. The compound with the best corrosion inhibition efficiency in 0.100 mol L^{-1} KCl solution was 1-PT. This behaviour is attributed to the packing density of this linear molecule compared to MPS and PTS that have bulky end groups compared to 1-PT.

Acknowledgements

The authors would like to acknowledge the financial support of the National Science Foundation (NSF)-EPSCoR Program, grant number (OSR 9 452 893) and to the Consejo Nacional de Investigación Científica y Tecnológica, CONICIT from Venezuela. The authors would like to acknowledge the Materials Characterization Center at UPR-Río Piedras.

References

1. G. TrabANELLI, in F. Mansfeld (Ed.), 'Corrosion Mechanisms' (Marcel Dekker, New York, 1987), p. 119.
2. K. Tatsuya, N. Hiroshi and A. Kunitsugu, *J. Electrochem. Soc.* **143** (1996) 3866.
3. A.N. Starchak, A.N. Krasovskii, V.A. Anishchenko and L.D. Kosukhina, *Zashch. Met.* **30** (1994) 405.
4. M.Th. Makhlof, S.A. El-Shatory and A. El-Said, *Mater. Chem. Phys.* **43** (1996) 76.
5. M.Th. Makhlof and M.H. Wahdan, *Pol. J. Chem.* **69** (1995) 1072.
6. M.Th. Makhlof, M.H. Wahdan and M. Hassan, *ACH-Models Chem.* **132** (1995) 903.
7. M.H. Wahdan, *Mater. Chem. Phys.* **49** (1997) 135.
8. Yu.I. Mikshis, L.A. Rastenite and A.I. Rutavichus, *Pot. Met.* **33** (1997) 288.
9. A. Srhiri, Y. Derbali and T. Picaud, *Corrosion* **51** (1995) 788.
10. S. Sankarapapavinasam and M.F. Ahmed, *J. Appl. Electrochem.* **22** (1995) 390.
11. G. Brunoro, A. Frignani and L. Tommesani, *Ann. Univ. Ferrara, Sez. Suppl.*, 10 (8th European Symposium on 'Corrosion Inhibitors', 1995, Vol. 2), (1995), p. 1053.
12. K. Mori and Y. Nakamura, *J. Polym. Sci. Polym. Lett. Ed.* **21** (1983) 889.
13. D.L. Seymour, S. Bao, C.F. McConville, M.D. Crapper, D.P. Woodruff and R.G. Jones, *Surf. Sci.* **189/190** (1987) 529.
14. J.Y. Gui, D.A. Stern, D.G. Frank, F. Lu, D.C. Zapien and A. Hubbard, *Langmuir* **7** (1991) 955.
15. J. Uehara and K. Aramaki, *J. Electrochem. Soc.* **138** (1991) 3245.
16. M.D. Porter, T.B. Bright, D.L. Allara and C.E.D. Chidsey, *J. Am. Chem. Soc.* **109** (1987) 3559.
17. G.M. Whitesides and P.E. Laibinis, *Langmuir* **6** (1990) 87.
18. M.M. Walczak, C. Chung, S.M. Stole, C.A. Widrig and M.D. Porter, *J. Am. Chem. Soc.* **113** (1991) 2370.
19. C.A. Widrig, C. Chung and M.D. Porter, *J. Electroanal. Chem.* **310** (1991) 335.
20. S.M. Stole and M.D. Porter, *Langmuir* **6** (1990) 1199.
21. P.E. Laibinis, G.M. Whitesides, D.L. Allara, Y.T. Tao, A.N. Parikh and R.G. Nuzzo, *J. Am. Chem. Soc.* **113** (1991) 7152.
22. P.E. Laibinis and G.M. Whitesides, *J. Am. Chem. Soc.* **114** (1992) 1990.
23. L.C.F. Blackman and M.J.S. Dewar, *J. Chem. Soc.* **195** (1990) 171.
24. M. Musiani, G. Mengoli, M. Fleischmann and R.B. Lowry, *J. Electroanal. Chem.* **217** (1987) 187.
25. M. Ohsawa and W. Suetaka, *Corros. Sci.* **19** (1979) 709.
26. G. TrabANELLI and V. Carassitti, in M.G. Fontana and R.W. Staehle (Eds), *Advances in Corrosion Science and Technology Vol. 1* (Plenum, New York, 1970), p. 147.
27. J.C. Marconato, L.O. Bulhes and M.L. Temperini, *Electrochim. Acta* **43** (1998) 771.
28. R. Haneda and K. Aramaki, *J. Electrochem. Soc.* **145** (1998) 1856.
29. R. Haneda, H. Nishihara and K. Aramaki, *J. Electrochem. Soc.* **144** (1997) 1215.
30. K. Suwa, T. Nishimoto, Y. Nagaoka and S. Aida, *Bull. Soc. Salt Sci. Jpn.* **15** (1961) 153.
31. Y. Yamamoto, H. Nishihara and K. Aramaki, *J. Electrochem. Soc.* **140** (1993) 436.
32. C. Miller, P. Cuendet and M. Grätzel, *J. Phys. Chem.* **95** (1991) 877.
33. C. Miller and M. Grätzel, *J. Phys. Chem.* **95** (1991) 5225.
34. Y. Yamamoto, H. Nishihara and K. Aramaki, *J. Electrochem. Soc.* **140** (1993) 2.
35. M. Itoh, H. Nishihara and K. Aramaki, *J. Electrochem. Soc.* **141** (1994) 8.
36. W.R. Thompson, M. Cai, M. Ho and J.E. Pemberton, *Langmuir* **13** (1997) 2291.
37. M. Itoh, H. Nishihara and K. Aramaki, *J. Electrochem. Soc.* **142** (1995) 6.
38. Y. Fend, W.-K. Teo, K.-S. Siow, Z. Gao, K.-L. Tan and A.-K. Hsieh, *J. Electrochem. Soc.* **144** (1997) 1.
39. H.P. Lee and K. Nobe, *J. Electrochem. Soc.* **133** (1986) 2035.
40. R. Tremont, H. De Jesús-Cardona, R.J. Castro and C.R. Cabrera, *J. Appl. Electrochem.* **30** (2000) 737.
41. R. Zvauya and J.L. Dawson, *J. Appl. Electrochem.* **24** (1994) 943.
42. L.H. Dubois and R.G. Nuzzo, *Annu. Rev. Phys.* **43** (1992) 437.
43. A. Morneau, A. Manivannan and C.R. Cabrera, *Langmuir* **10** (1994) 3940.
44. J. Wood and R. Sharman, *Langmuir* **10** (1994) 2307.
45. G. Che and C.R. Cabrera, *J. Electroanal. Chem.* **417** (1996) 155.
46. G. Che, A. Manivannan and C.R. Cabrera, *Physica A* **231** (1996) 304.
47. S.K. Jung and G.S. Wilson, *Anal. Chem.* **68** (1996) 591.
48. M. Itoh, H. Nishihara and K. Aramaki, *J. Electrochem. Soc.* **142** (1995) 3696.
49. W.R. Thompson and J.E. Pemberton, *Chem. Mater.* **7** (1995) 1309.
50. W.R. Thompson, M. Cai and J.E. Pemberton, *Langmuir* **13** (1997) 2291.
51. G. Che, H. Zhang and C.R. Cabrera, *Electroanal. Chem.* **453** (1998) 9.

52. W.R. Thompson, M. Cai, M. Ho and J.E. Pemberton, *Langmuir* **13** (1997) 2291.
53. M. Itoh, H. Nishihara and K. Aramaki, *J. Electrochem. Soc.* **142** (1995) 6.
54. Y. Fend, W.-K. Teo, K.-S. Siow, Z. Gao, K.-L. Tan and A.-K. Hsieh, *J. Electrochem. Soc.* **144** (1997) 1.
55. H.P. Lee and K. Nobe, *J. Electrochem. Soc.* **133** (1986) 2035.
56. S. Sankarapavinasam and M.F. Ahmed, *J. Appl. Electrochem.* **22** (1990) 390.
57. G. Quartarone, G. Moretti, T. Bellomi, G. Capobianco and A. Zingales, *Corrosion* **54** (1998) 606.
58. J.O'M. Bockris and D.A.J. Swinkels, *J. Electrochem. Soc.* **111** (1964) 736.
59. E. Kamis, *Corrosion* **46** (1990) 478.
60. A.N. Frumkin and B.B. Damanskin, in J.O'M. Bockris, B.E. Conway (Eds), 'Modern Aspects of Electrochemistry', Vol. 3, (Butterworths, London, 1964), p. 152.
61. B.G. Ateya, B.E. El-Anadouli and F.M. El-Nizami, *Corros. Sci.* **24** (1984) 509.
62. R. Zvauya and J.L. Dawson, *J. Appl. Electrochem.* **24** (1994) 943.
63. E. Kamis, F. Bellucci, R.M. Latanision and E.S.H. El-Ashry, *Corrosion* **47** (1991) 677.
64. F.M. Donahue and K. Nobe, *J. Electrochem. Soc.* **112** (1965) 886.